Pergamon

0042-6989(95)00279-7

Vision Res., Vol. 36, No. 4, pp. 605–612, 1996

0042-6989/96 $15.00 + 0.00

Research Note

Sub-pixel Accuracy: Psychophysical Validation of an Algorithm for Fine Positioning and Movement of Dots on Visual Displays

MARK A. GEORGESON,*† TOM C. A. FREEMAN,*‡ NICHOLAS E. SCOTT-SAMUEL*†

Received 24 January 1995; in revised form 18 May 1995

Many visual experiments call for visual displays in which dots are plotted with very fine positional accuracy. Spatial hyperacuities and motion displacement thresholds can be as low as 5 sec arc. On computer graphics displays small angular displacements of a pixel can be obtained only with long viewing distances which impose a small field of view. To overcome this problem, we describe a method for positioning the centroid of a *quadrel* (a 2 × 2 block of pixels) with very high accuracy, equivalent to 0.4% of a pixel width. This enables dot displays to be plotted with high positional accuracy at short viewing distances with larger fields of view. We show psychophysically that hyperacuities can be measured with sub-pixel accuracy in quadrel displays. Motion displacement thresholds of 16 sec arc were measured in multiple-dot and single-dot displays even though the pixel spacing was 1.2 min arc. Quadrel displays may be especially useful in studies of optic flow and structure-from-motion which demand a fairly large field of view along with fine positional accuracy.

Visual displays Dots Hyperacuity Motion thresholds Pixels Centroids

INTRODUCTION

Many areas of visual experimentation call for visual displays in which dots are plotted with very fine positional accuracy. Studies of spatial hyperacuities—e.g. vernier acuity, three-dot alignment, interval bisection tasks—make great demands on the display because discrimination thresholds can be as small as 5 sec arc (e.g. Andrews, Butcher & Buckley, 1973; Westheimer & McKee, 1977b) or less (Klein & Levi, 1985). Stereo and motion thresholds can also be just as fine as spatial hyperacuity (McKee, Welch, Taylor & Bowne, 1990). The lower threshold of motion for gratings in foveal vision is about 0.02 deg/sec, irrespective of spatial frequency (Harris, 1984; Johnston & Wright, 1985), so that at a typical frame rate of 60 Hz the spatial displacement per frame would need to be as small as 1.2 sec arc. Even reducing the refresh rate to (say) 15 Hz would still demand 5 sec arc displacement per frame. Accurate portrayal of structure-from-motion in moving dot patterns also demands such fine positioning of dots on a display. In the last 20 yr computer-generated displays have brought many advantages to vision research, but fine positioning of dots is not one of them. A typical graphics card and 14 in. computer monitor plots points in a 640 × 480 array, with pixels spaced at 0.37 mm intervals. To make these intervals subtend 5 sec arc requires a viewing distance of 15 m. This is not only inconvenient, to say the least, but reduces the overall display size to less than 1 deg. The most expensive high-resolution displays improve on this situation, but only by about a factor of 2.

Thus for many reasons the ability to plot points with a positional accuracy much better than 1 pixel would be very desirable. For one-dimensional images there is a neat solution (Morgan & Aiba, 1985) based upon the idea that, because of optical blur, two adjacent lines (i.e. two adjacent columns of pixels) give very nearly the same retinal light distribution as a single line placed at the centroid of the line-pair (Westheimer & McKee, 1977a; Watt & Morgan, 1983). When the relative intensity of the two lines is varied, the centroid moves smoothly in the interval between the two component lines. Hence the effective position of the (unresolved) line-pair can be positioned with arbitrary accuracy by varying the relative intensity of the component lines. The brightness can be held constant by holding the sum of the two intensities constant. Recently, Morgan, Ward and Cleary (1994) showed psychophysically that motion displacement

*Department of Vision Sciences, Aston University, Birmingham B4 7ET, England [*Email* m.a.georgeson@bham.ac.uk].
†Present address: School of Psychology, University of Birmingham, Birmingham B15 2TT, England.
‡Present address: School of Optometry, University of California, Berkeley, CA 94720, U.S.A.

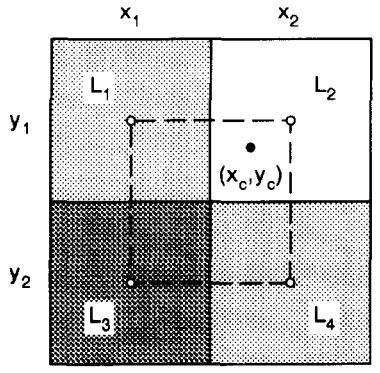

FIGURE 1. A quadrel is the set of four pixels that surround the desired dot location (X_c, Y_c). When viewing distance and optical blur ensure that the quadrel is effectively an unresolved 'dot' then its effective location is at the centroid of the four pixels. By adjusting the pixel intensities L_1–L_4 we can steer the centroid to any desired location within the dashed square, thus giving very high accuracy in the plotting of 'dots' in a display.

thresholds for such line-pairs are indeed determined by the displacement of the centroid.

From one dimension to two dimensions

In this paper, we consider the problem of extending the method to two-dimensional images: how can a 'dot' be positioned with great accuracy in the x–y plane of a pixellated display? To position the centroid *between* pixels on both the x and y axes, the 'dot' must clearly be at least a 2 × 2 group of pixels. We shall refer to such a group as a *quadrel*, since it is composed of 4 pixels that form the smallest plotting element with this method. The problem can now be stated more precisely: how can we determine the intensities of the 4 pixels within a quadrel, such that the centroid of the quadrel is placed at any desired (x, y) location? Intriguingly, this extension of the method from one to two dimensions turns out to be far from trivial. In one dimension the problem of choosing the two pixel (line) intensities has a simple, unique solution. In two dimensions there is no unique solution, and some of the multiple solutions are 'illegal' in the sense that they call for negative pixel intensities. For example, if we want to place the centroid at the centre of the quadrel, then setting the intensity values L_1, L_2, L_3, L_4 (see Fig. 1) to 1,1,1,1 would do so. Setting the values to 3, −1, −1,3 would also do so, but it would be 'illegal'. We offer an algorithm for rapid computation of the four intensities that is always 'legal' and greatly improves the spatial accuracy of dot displays and the smoothness of motion in moving dot sequences. The cost of this improvement is that spatial *resolution* within one frame is halved. We cannot allow quadrels to overlap and so the quadrel spacing must be twice the pixel spacing. This will not be a problem for many experimental applications where dots are relatively sparse.

THEORY

Finding the four intensities

Let the desired location of the quadrel's centroid be X_c, Y_c. The four pixel locations that surround the centroid are easily found (see Fig.1):

$$x_1 = \mathrm{INT}(X_c),\ x_2 = x_1 + 1, \tag{1a}$$

$$y_1 = \mathrm{INT}(Y_c),\ y_2 = y_1 + 1, \tag{1b}$$

where INT(x) is the nearest integer $\leqslant x$. Let their intensities be L_1, L_2, L_3, L_4, as shown in Fig. 1. We assume for the moment that the background intensity is zero, and we consider later what happens when it is non-zero. To keep the brightness of the 'dot' constant let the sum $L_1 + L_2 + L_3 + L_4$ be a constant, L. The centroid is then defined by:

$$X_c = (L_1 \cdot x_1 + L_2 \cdot x_2 + L_3 \cdot x_1 + L_4 \cdot x_2)/L \text{ and} \tag{2a}$$

$$Y_c = (L_1 \cdot y_1 + L_2 \cdot y_1 + L_3 \cdot y_2 + L_4 \cdot y_2/L. \tag{2b}$$

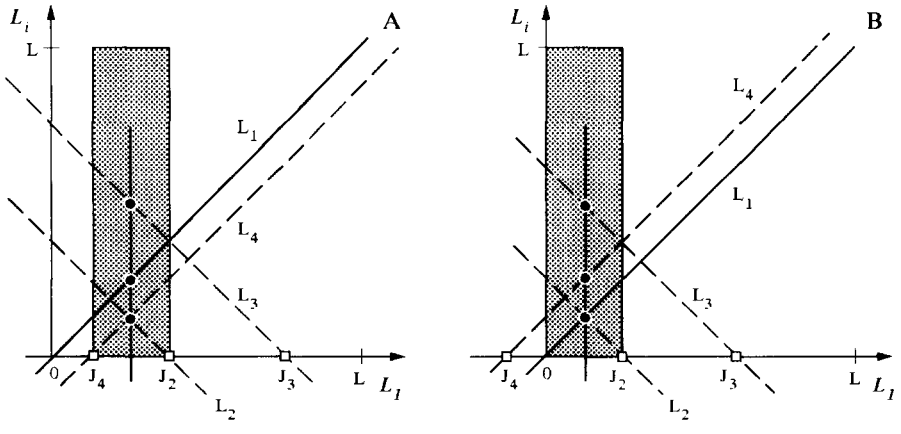

FIGURE 2. Graphical representation of the solution to the problem of finding the pixel intensities (L_1, L_2, L_3, L_4) that yield a given centroid. Equations 3(a, b, c) show that each of the intensities L_2, L_3, L_4 is a linear function of L_1. Thus choosing a value for L_1 determines the other three values. (A, B) The shaded region indicates the range of values of L_1 that ensures $L_2, L_3, L_4 \geqslant 0$, and the solid vertical line indicates a particular chosen solution. These panels show two examples, for two different centroids, where the L_4 function intersects the L_1 axis at a positive value (A) or a negative value (B)—see equations (6a, b).

Manipulating these equations yields:

$$L_2 = L(1 - Y_c + \mathrm{INT}(Y_c)) - L_1, \quad (3a)$$

$$L_3 = L(1 - X_c + \mathrm{INT}(X_c)) - L_1, \quad (3b)$$

$$L_4 = L - (L_1 + L_2 + L_3). \quad (3c)$$

Thus both L_2 and L_3 are linear functions of L_1 with a slope of -1. Let $J_2 = L(1 - Y_c + \mathrm{INT}(Y_c))$, $J_3 = L(1 - X_c + \mathrm{INT}(X_c))$. J_2 and J_3 represent the values of L_1 at which the two functions L_2, L_3 meet the L_1 axis, and are constant for a given centroid. We then have:

$$L_2 = J_2 - L_1 \quad (4a)$$

$$L_3 = J_3 - L_1 \quad (4b)$$

$$L_4 = L - J_2 - J_3 + L_1. \quad (4c)$$

Equations (4a, b, c) represent constraints on the choice of the four pixel intensities, illustrated in Fig. 2. L_4 is also a linear function of L_1 with a slope of +1. Given the desired centroid (X_c, Y_c) and the desired intensity (L), a legal solution is given by any choice of L_1 that yields $L_i \geq 0$, for $i = 1,2,3,4$. The shaded region in Fig. 2 depicts the range of L_1 for which legal solutions exist, and a solution can be found graphically by drawing a vertical line through this region and finding where it intersects the four functions (L_1–L_4). The solid symbols show the set of four intensities obtained by choosing L_1 to lie in the centre of the solution region. Let the L_4 function meet the L_1 axis at J_4. Then

$$J_4 = J_2 + J_3 - L. \quad (5)$$

In general, $0 \leq J_2 \leq L$, $0 \leq J_3 \leq L$, and $-L \leq J_4 \leq L$. Given the constraint that all intensities must be ≥ 0, and letting $J_{\min}$ be the lower of the values J_2 and J_3, we can define the solution region formally as:

$$J_4 \leq L_1 \leq J_{\min} \ (\text{if } J_4 \geq 0), \quad (6a)$$

$$0 \leq L_1 \leq J_{\min} \ (\text{if } J_4 < 0). \quad (6b)$$

These two cases are illustrated in Fig. 2(A, B) respectively. We have no strong criteria for choosing one solution over another, but we note that the average of all possible solutions is obtained simply by choosing L_1 to lie in the centre of the solution region. With this choice we get:

$$L_1 = (J_{\min} + J_4)/2 \ (\text{if } J_4 \geq 0), \text{ or} \quad (7a)$$

$$L_1 = J_{\min}/2 \ (\text{if } J_4 < 0). \quad (7b)$$

Inserting this value of L_1 into the expressions for L_2, L_3, L_4 yields four intensities that define a quadrel with the desired centroid and intensity. (See Discussion for an alternative choice of solution.)

Non-zero background intensity

What are the pixel 'intensities' that enter into the centroid calculation? When the background intensity $I_0 > 0$, the values L_i could represent absolute intensity which we denote by I_i, or incremental intensity ($I_i - I_0$), or local contrast $(I_i - I_0)/I_0$. The second and third of these options give the same centroid as each other, but it is different from that given by absolute intensity. Morgan and Aiba (1985) discussed this issue in the one-dimensional case and showed that for vernier acuity the centroid position was determined by incremental intensity (or contrast), not by absolute intensity. Using this result, we can compute L_i as for the zero background case, and then to obtain the absolute pixel intensities (I_i), set $I_i = (I_0 + L_i)$ to plot increments (light dots), or $I_i = (I_0 - L_i)$ to plot decrements (dark dots). Importantly, with these definitions $L_i \geq 0$ for both increments and decrements, and the centroid of an asymmetric quadrel does not change if its contrast is reversed. The calculations are not elaborate, and so quadrel plotting is quick and efficient.

In the next section we describe some experiments designed to validate the proposed method. The experiments serve as an example that motion displacements as small as (say) 0.16 min arc can be tested (and discriminated by human vision) even though the pixels subtended 1.2 min arc at a viewing distance of 69 cm.

EXPERIMENTS

General methods

We measured the lower threshold of motion (LTM) and step displacement thresholds (often called $D_{\min}$) for an array of 64 achromatic dots. The image sequences were computed by a Dell 486DX computer, written into the 4 MB framestore of a Cambridge Research Systems VSG2/2, and displayed on an Eizo 15 in. colour monitor at a frame rate of 90 Hz (frame duration 11.1 msec). Linearization of the relation between digital signal value and displayed luminance ('gamma correction') was achieved to high accuracy ($r^2 = 0.99937$), by manipulating the content of the look-up tables. Calibrations were carried out with a Minolta LS110 digital photometer, plotting the luminance of a small central patch (50×50 pixels) as a function of pixel value (0–255). We have found that display monitors exhibit non-linear spatial interaction, in that the luminance gain for the central test patch increased somewhat with the intensity presented in the surrounding region. This was not due to light scatter in the tube, nor in the photometer, since it was a multiplicative not an additive effect. In general it is safest to calibrate the monitor under conditions close to those to be used experimentally. We set the background pixels to their minimum value and linearized the light output for this condition.

The spatial array of dots was quasi-random, in the

sense that each dot was confined within its own cell of an 8 × 8 square array, but the dot's location in that cell was chosen randomly within a central square whose width was half the width of the cell. The cells were 64 pixels (75 min arc) wide, and so the average spacing between dots was also 75 min arc. The minimum spacing was 38 min arc. The background intensity was set to minimum (0.54 cd/m^2) while the quadrel intensity L (the sum of the four pixel intensities) was equivalent to the maximum intensity available from a single pixel. A packed array of such pixels had a luminance of 113 cd/m^2. The intensity of dots around the borders of the array was smoothed off by a circular window function whose edge profile was half a cycle of a raised cosine (half-period 50 pixels). The diameter of the window function at half-height was 400 pixels (7.8 deg). It was always stationary, and prevented the undesirable twinkling of dots as they appeared or disappeared around the edges during a movement of the array.

The LTM

Procedure. To study LTM the display was a simulated sample of continuous movement rather than a single step displacement. A small, central, red fixation point (2 × 2 pixels) appeared 500 msec before the onset of the dot array and remained on until the offset of the array. The dot display lasted for 45 frames (500 msec). The positions of the dots were updated every 3 frames (33.3 msec) to produce slow movements to the left or right. The subject's task was to report the direction of movement. Twelve speeds were tested in the range ±0.0367 deg/sec. Both quadrel and pixel displays were tested, with integer start positions. Quadrels were plotted with their centroids at the desired locations using the method described above. Pixel positions had to be rounded to the nearest integer, and this meant that for pixels no actual displacements occurred at all for speeds lower than 0.02 deg/sec.

Viewing was binocular in a darkened room, at a distance of 69 cm from the screen, with the head stabilized by a chin and forehead rest. Each observer performed a total of 60 randomly ordered trials for each speed of displacement. Feedback was given as a 'beep' after each incorrect response. Separate sessions testing quadrel and pixel displays were interleaved during the experiment. Two observers (authors TCAF and NESS) with normal, corrected vision were tested.

Results. The results are shown in Fig. 3, pooled across the two observers. For the quadrel display we obtained a smooth psychometric function. The threshold speed (LTM), defined conventionally as the distance between the 50% and 75% points, was 0.017 deg/sec or 1.0 min arc/sec. This is very similar to previous results obtained with gratings, described above (Harris, 1984; Johnston & Wright, 1985). At the threshold speed, the dots moved through 0.5 min arc during the 500 msec interval, somewhat further than the 0.27 min arc threshold obtained for step displacement (below). The pixel display was unable to present such low speeds, and performance was necessarily at chance below 0.02 deg/sec.

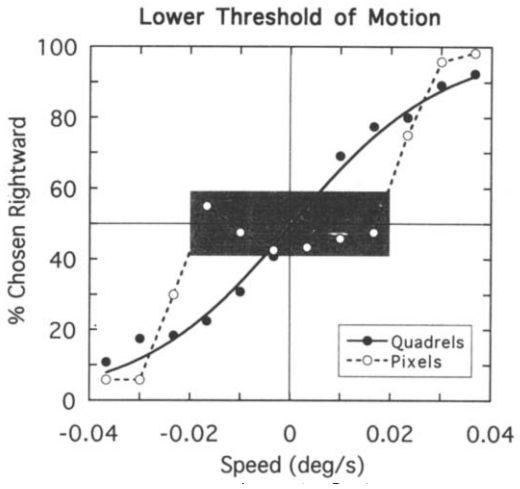

FIGURE 3. Lower threshold of motion tested on pixel and quadrel displays composed of 64 dots with integer start positions. Observers had to report the direction of movement (left or right). Data pooled across two observers (TCAF, NESS; total $n = 120$ trials/point). For quadrels (●) 0.017 deg/sec was the slowest speed of movement for which direction could be discriminated at the 75% level. For pixels (○) performance was at chance up to ±0.02 deg/sec because rounding the dot position to the nearest pixel position meant that no actual displacement occurred. These chance results fall in the shaded region which shows a range of ±2 SDs of the sampling distribution for binomial samples of size $n = 120$ and chance performance, $p = 0.5$.

Step displacement detection

To measure displacement detection the procedure, apparatus and characteristics of the display were in most respects the same as for the experiment on LTM. The dot array was presented for 46 frames (511 msec). It remained stationary for the first 23 frames, then stepped abruptly through a small distance, and remained stationary again. The subject's task was to report the direction of displacement (left/right, or up/down, in different sessions). The displacements were ±0.16, 0.48 and 0.80 min arc. As before, a red fixation point appeared for 500 msec before the onset of the dots and was held on until the offset of the dots. Three observers (the authors) with normal, corrected vision were tested.

Results. Figure 4(A, B) presents results as psychometric functions pooled across the three observers ($n = 180$ trials per point), for horizontal displacements. In Fig. 4(A) we compare performance with dots made from quadrels and from single pixels. For quadrels we obtained a smooth psychometric function and the threshold displacement was 0.27 min arc, or 16 sec arc. This is similar to the results of Snowden (1992) who found displacement thresholds of 20 sec arc under fairly similar conditions using an analogue display with 400 dots presented for 200 msec. Random-dot displacement thresholds as low as 8–14 sec arc were reported by Hadani, Gur, Meiri and Fender (1980), but it may be important that their observers were allowed to scrutinize a continuously oscillating display, and had to detect only the presence of oscillation, not report direction of

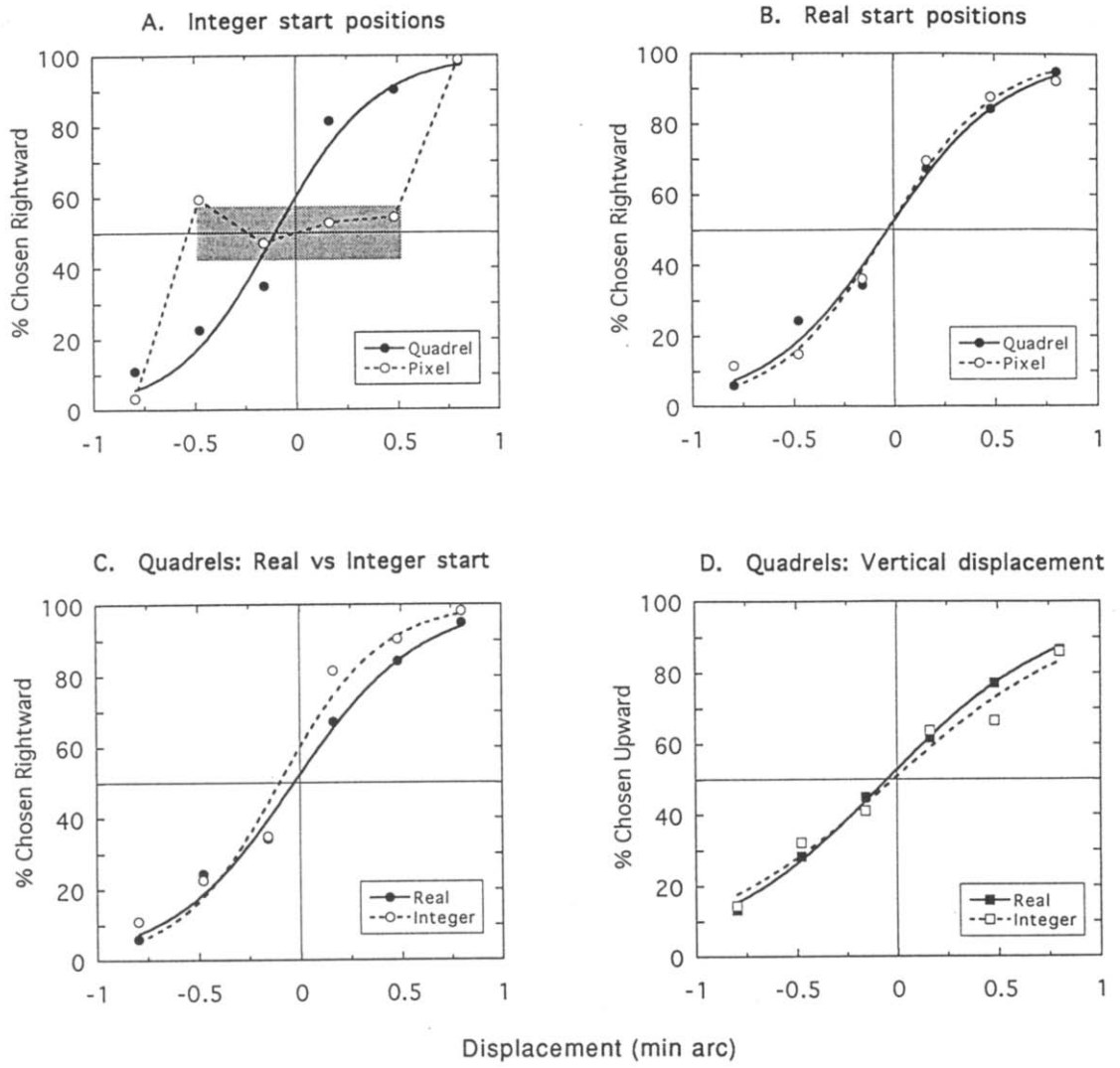

FIGURE 4. Validation of the quadrel method by psychophysical testing of displacement sensitivity. The array of 64 dots was subject to a small step displacement to the left or right. Observers had to report the direction of displacement. Data pooled across three observers (total $n = 180$ trials per point). (A) Integer start positions: all dots in the first frame were centred on a pixel position. The smooth psychometric function for quadrels (●, fitted by a logistic function) indicates a threshold displacement of 0.27 min arc. The pixel display (○) necessarily shows chance performance for 'displacements' up to $\frac{1}{2}$ a pixel width since the dot positions were rounded to the nearest pixel position and no actual displacement took place. Pixel width was 1.2 min arc. The shaded region, as in Fig. 3, is where most chance results should fall. (B) With real-valued start positions (see text) performance on pixels and quadrels was similar. This result does *not* mean that the pixel display accurately portrays small step displacements, since the pixel displacements were probabilistic. (C) Quadrels only. Integer and real start positions compared directly [data reproduced from (A) and (B)]. Slightly higher performance for rightward displacements and integer start positions was probably an artefact of the 'adjacent pixel non-linearity' (see text), since it was absent for vertical displacements (D).

movement. All these factors would tend to improve performance.

With pixel displays (as opposed to quadrels), there are two distinct ways to do the experiment. If the initial set of points has integer-valued co-ordinates and the displaced locations are rounded to the nearest pixel position, then no actual displacement occurs at all for nominal displacements up to 0.6 min arc ($\frac{1}{2}$ a pixel), whereas a nominal displacement between a $\frac{1}{2}$ and 1 pixel would actually jump 1.2 min arc (1 pixel). Figure 4(A) (open symbols) confirms the expected outcome. Chance performance for nominal displacements less than $\frac{1}{2}$ a pixel suddenly switched to near-perfect performance at a greater nominal displacement (0.8 min arc). These data highlight the limitations of a pixellated display.

The second way of plotting the pixels is more subtle: the initial and final positions of each dot are calculated as real values, and then rounded to the nearest pixel position for plotting. This means that for small nominal displacements, some points jump through 1 pixel position, while others remain stationary. Let the desired (nominal) displacement be d, and the separation between pixels be p, with $0 \leqslant d \leqslant p$. On average the proportion of points that do jump will be (d/p) and the average displacement of the set of points is d. Figure 4(B) shows that performance with this pixel display was strikingly

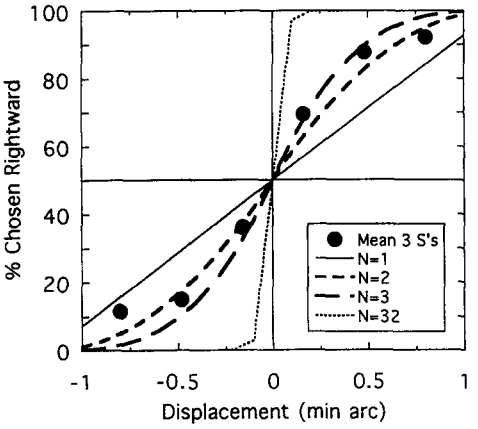

FIGURE 5. Pixel data [from Fig. 4(B)] compared with predictions of probability summation over N dots (N = 1,2,3 or 32), on the assumption that a single pixel jump will always be seen. This analysis suggests only two or three dots contributed significantly to performance.

similar to the quadrel display. For pixels it was the *probability* of a displacement that varied while for quadrels the *size* of the displacement varied. Why should these two manipulations yield almost identical performance?

On the face of it, this is a scientific question beyond the scope of a methodological paper. Nevertheless, the aim of this paper was to show the practical advantages to be gained from quadrel displays. Figure 4(B) apparently does not do so, since pixel and quadrel performances were the same, even though the objective, space–time structure and subjective appearance of the two types of movement were quite different. We felt constrained to pursue the issue further.

One possibility is that the motion of individual dots is detected independently, with probability summation over N dots contributing to the overall level of performance. If we assume that the displacement of 1 dot through 1 pixel width is always detectable, then for the pixel display it is straightforward to predict the psychometric function from first principles, with N as a parameter. The probability that any given dot undergoes a displacement is d/p (see above). Hence the probability that none of the N dots moves is $(1 - d/p)^N$. When no dot moves, the subject must guess with probability 0.5, and the probability of a correct response $P(C)$ is:

$$P(C) = 1 - 0.5(1 - d/p)^N. \quad (8)$$

In Fig. 5 this function is used to plot the probability of a rightward response $P(R)$ for several values of N. [To calculate $P(R)$ for leftward steps, $d < 0$, take the absolute value of d and let $P(R) = 1 - P(C)$.] The pixel data are fairly well modelled by a value of N somewhere between 2 and 3. This model assumes that observers detected 1-pixel displacements perfectly, and independently, but only processed 2 or 3 dots in the display. This could mean that the greatest contribution to detection was made by the few dots that lay closest to the fixation point, with much lower sensitivity to displacements of the more peripheral dots in the display. This is fairly plausible since even the closest dots had an average eccentricity of 53 min arc.

Now we can address the similarity of pixel and quadrel performance. Suppose probability summation occurred over N dots in the same way for pixel and quadrel displays. The similarity in performance for the multi-dot displays would then have to be a consequence of similar detectabilities for single-dot displacements. When $N = 1$,

$$P(C) = 0.5(1 + d/p). \quad (9)$$

That is, the psychometric function for the probabilistic displacement of a single pixel should be a linear function

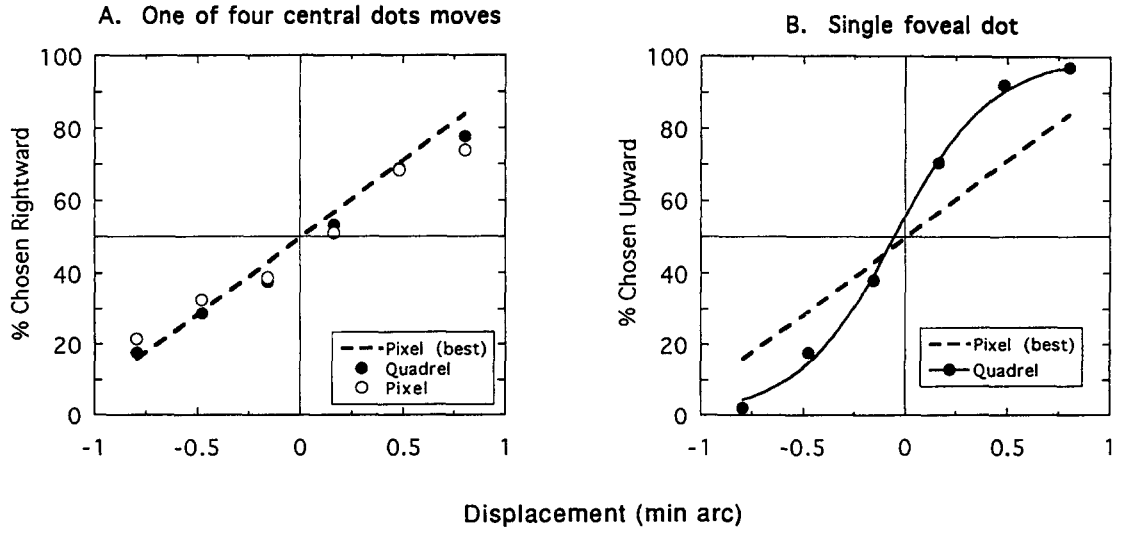

FIGURE 6. Single dot displacements. (A) A replication of the experiment shown in Fig. 4(B), except that only one of the 64 dots moved. The dot that moved could be any one of the four dots closest to the fixation point. As in Fig. 4(B), start positions were real and displacements horizontal. For quadrels, the centroid stepped through displacement ($\pm d$) shown on the abscissa. For pixels, the dot stepped through 1 pixel width, with probability (d/p) where p is the pixel width (1.2 min arc). (B) Detection of vertical displacement of a single quadrel presented at the fovea. Dashed lines in (A) and (B) show the best possible performance obtainable for the pixel condition. Symbols: means of three observers; total n = 180 trials/point.

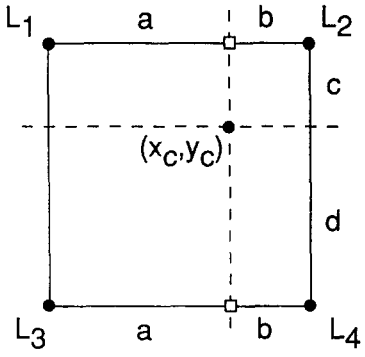

FIGURE 7. A simple, alternative rule for finding the four pixel intensities (B. Backus, personal communication). Each intensity is set proportional to the area of the quadrant opposite to it. Thus $L_1 = b \cdot d \cdot L$, $L_2 = a \cdot d \cdot L$ etc., where $L = L_1 + L_2 + L_3 + L_4$, $a + b = c + d = 1$. See Discussion for details of derivation.

of the nominal displacement, d. We tested this experimentally, and asked whether a similar linear function would be obtained for displacement of a single quadrel.

Single dot displacements. We repeated the experiment of Fig. 4(B), except that only one of the 64 dots moved. The dot that moved could be any one of the four dots closest to the fixation point. As before, the start positions were real and displacements were horizontal. For quadrels, the centroid of the dot stepped through a variable displacement ($\pm d$, $d > 0$) while for pixels, rounding the dot location to the nearest pixel position meant that the dot stepped through 1 pixel width with probability (d/p) or it was stationary with probability ($1 - d/p$). Figure 6(A) shows the results, pooled over the three subjects as before. Performance on both displays lay close to the linear function expected for pixels. This function (dashed line) represents the best possible performance for a single pixel, since it is based simply on the assumption that whenever the pixel actually jumps its direction is always seen correctly.

For quadrels we can see no reason in principle why this line should constrain performance. For example, if the experiment had been done at smaller retinal eccentricities performance (as we show below) would have been better for the quadrel, but could not have been better for the pixel. We must conclude, surprisingly, that the similarity for single dot displacements is largely accidental, perhaps depending on the particular eccentricities used, and that the similarity for multiple dots is a consequence of this.

To be confident of this conclusion, we ran one further experiment with a single quadrel presented foveally. Procedures were as before, except that the 64-dot array was replaced by a single quadrel at the centre of the display, and the single fixation point was replaced by four white pixels placed at the corners of an imaginary square. The width of this four-dot fixation square was 32 pixels (38 min arc), and the test dot appeared at its centre. Observers fixated the centre of the square to place the test dot at the centre of the fovea. Displacement was vertical. Figure 6(B) shows that performance on this single quadrel was substantially better than the upper limit for a single pixel. The average threshold was 16 sec arc, about the same as the non-foveal, multi-dot display [Fig. 4(C)]. The main points we draw from this experiment are that there is no overall fixed relationship between quadrel and pixel performance, and that much finer performance can be tested and measured with quadrels than with pixels.

For the multi-dot displacements [Fig. 4(B)] we considered a second possibility: that responses to local speeds or displacements are averaged by the visual system over wider regions of space, and that subjects' decisions are based on this averaged response. Since the mean displacement (averaged across space) is the same for the pixel and quadrel displays the similarity of performance is directly predicted. Evidence for broad spatial pooling of signals in direction discrimination has been reported by Watamaniuk and Sekuler (1992). However, the similarity between pixel and quadrel performance even for single dot displacements [Fig. 6(A)] makes the spatial pooling explanation of our data [Fig. 4(B)] much less likely.

The smooth functions obtained for pixels in Figs 4(B) and 6(A) are essentially a statistical artefact, since the procedure varies the probability of a jump instead of varying the size of the jump. This is not a procedure one would normally want to adopt, and the 'roughness' of the velocity distribution would often be quite unsuitable, e.g. in studies of optic flow where smooth velocity gradients are required. The more revealing comparisons are surely those shown in Figs 3 and 4(A) where the sub-pixel capabilities of the quadrel display are clearly shown.

DISCUSSION

A complication: adjacent pixel non-linearity

Ideally the brightness of pixels and quadrels should have been the same, since the sum L of the four intensities in the quadrel was set equal to that of a single pixel. We noticed, however, that quadrels often tended to look brighter than single pixels. With displacement from an integer start position the dot starts as a pixel but transforms into a quadrel, and for horizontal (but not vertical) movements this was accompanied by a visible brightening. We think this is a consequence of nonlinear spatial interaction between adjacent pixels inherent in most CRT displays (Mulligan & Stone, 1989). In a display that scans horizontally, the luminous output of a pixel is affected by neighbouring pixels that are horizontally adjacent, and in an extreme case the mean luminance of a high frequency vertical grating on such a display can be dramatically lower than that of a horizontal grating on the same display. Mulligan and Stone (1989) found that the effect could be well described by assuming low-pass filtering of the video signal in the monitor before the non-linear ('gamma function') relationship between Z-voltage and luminance output. The brightening effect may have had a small influence on our data, since it can be seen that performance on rightward displacements was slightly better for integer start positions than for real ones [Fig. 4(C)], but there was

no such effect for vertical displacements [Fig. 4(D)]. Subjectively, the variation in brightness was not noticeable for real start positions where it is randomized across the set of dots. It was not visible, nor would it be expected, for vertical displacements. Nevertheless it is a potential artefact in the quadrel method, and we look forward to the publication of algorithms for look-up tables to compensate for it (Klein, Carney & Hu, 1996; Klein, Hu & Carney, 1996).

Choice of solutions

Our routine for computing quadrel intensity values opted for the centre of the solution region (Fig. 2). After this paper was submitted we learned of another rule that is simple and neat (B. Backus, personal communication). It adds one further constraint to the solution by assuming that the centroid of the pair of points (L_1, L_2) lies at (X_c, y_1), from which it follows that the centroid of (L_3, L_4) must lie similarly at (X_c, y_2) (□ in Fig. 7). Suppose that X_c divides the interval (x_1, x_2) in the ratio $a:b$ (Fig. 7), and similarly Y_c divides the interval (y_1, y_2) in the ratio $c:d$ (i.e. $b = x_2 - X_c$, $a = 1 - b$, $d = y_2 - Y_c$, $c = 1 - d$). Equations (3a, b) can be re-written as:

$$L_2 = L \cdot d - L_1, \tag{10a}$$

$$L_3 = L \cdot b - L_1. \tag{10b}$$

It follows from the new constraint that

$$L_1 \cdot a = L_2 \cdot b, \tag{11a}$$

$$L_1 \cdot c = L_3 \cdot d. \tag{11b}$$

Simple manipulation yields

$$L_1 = b \cdot d \cdot L,\ L_2 = a \cdot d \cdot L,\ L_3 = b \cdot c \cdot L,\ L_4 = a \cdot c \cdot L. \tag{12}$$

This rule necessarily delivers values falling within the solution space of Fig. 2, and in the examples shown there it would be represented by a solution line lying to the right of the centre line used in this paper. However, it is clearly easier to think about this solution in the geometry of Fig. 7. Each intensity is proportional to the area of the quadrant opposite to it.

What is gained from quadrels?

This paper offers a useful and practical method for accurately positioning dots on a computer screen, by generalizing the one-dimensional method of Morgan and Aiba (1985). With the use of quadrels the accuracy is not limited by pixel size. The ultimate limit on centroid positioning is set by the grey-level resolution of the display, since the smallest movement of a quadrel occurs when just one of its four pixels changes by one grey-level. With an 8-bit system (256 grey levels) the minimum displacement is 0.4% of a pixel width, 0.3 sec arc in our experiments. This is an order of magnitude better than required for the finest hyperacuities. Viewing distances can thus be shorter and the angular size of the display can be much larger than with a pixel display. One limit to the possible improvement is that if the viewing distance is too short then the internal structure of the quadrel will be resolved, and its status as a "dot" becomes questionable [see Morgan *et al.* (1994) for further discussion of the one-dimensional case]. If elements larger than 2 × 2 pixels are required, quadrels can simply be abutted to form the desired size and shape. A common displacement of all the quadrel centroids moves the global shape in the same way. The quadrel method may be particularly useful for experiments on optic flow and structure-from-motion that demand both a large display and accurate displacement of dots.

REFERENCES

Andrews, D. P., Butcher, A. K. & Buckley, B. R. (1973). Acuities for spatial arrangement in line figures: Human and ideal observers compared. *Vision Research, 13*, 599–620.

Hadani, I., Gur, M., Meiri, A. Z. & Fender, D. H. (1980). Hyperacuity in the detection of absolute and differential displacements of random dot patterns. *Vision Research, 20*, 947–951.

Harris, M. G. (1984). The role of pattern and flicker mechanisms in determining the spatiotemporal limits of velocity perception. 2. The lower movement threshold. *Perception, 13*, 409–415.

Johnston, A. & Wright, M. J. (1985). Lower thresholds of motion for gratings as a function of eccentricity and contrast. *Vision Research, 25*, 179–185.

Klein, S. A. & Levi, D. M. (1985). Hyperacuity thresholds of 1 sec: Theoretical predictions and empirical validation. *Journal of the Optical Society of America A, 2*, 1170–1190.

Klein, S. A., Carney, T. & Hu, Q. J. (1996). Improved lookup table to correct CRT pixel nonlinearity. In Rogowitz, B. E. & Allenbach, J. P. (eds) *Human vision, visual processing and digital display VI*. In press.

Klein, S. A., Hu, Q. J. & Carney, T. (1996). The adjacent pixel nonlinearity: Problems and solutions. Submitted.

McKee, S. P., Welch, L., Taylor, D. G. & Bowne, S. F. (1990). Finding the common bond: Stereoacuity and the other hyperacuities. *Vision Research, 30*, 879–891.

Morgan, M. J. & Aiba, T. S. (1985). Vernier acuity predicted from changes in the light distribution of the retinal image. *Spatial Vision, 1*, 151–161.

Morgan, M. J., Ward, R. M. & Cleary, R. F. (1994). Motion displacement thresholds for compound stimuli predicted by the displacement of centroids. *Vision Research, 34*, 747–749.

Mulligan, J. B. & Stone, L. S. (1989). Halftoning method for the generation of motion stimuli. *Journal of the Optical Society of America A, 6*, 1217–1227.

Watamaniuk, S. N. J. & Sekuler, R. (1992). Temporal and spatial integration in dynamic random-dot stimuli. *Vision Research, 32*, 2341–2347.

Watt, R. J. & Morgan, M. J. (1983). Mechanisms responsible for the assessment of visual location: Theory and evidence. *Vision Research, 23*, 97–109.

Westheimer, G. & McKee, S. P. (1977a). Integration regions for visual hyperacuity. *Vision Research, 17*, 89–93.

Westheimer, G. & McKee, S. P. (1977b). Spatial configurations for visual hyperacuity. *Vision Research, 17*, 941–947.

Acknowledgements—We thank Tim Meese and Mike Harris for commenting on the manuscript, Ben Backus (School of Optometry, Berkeley, Calif. U.S.A.) for the solution of Fig. 7 and the BBSRC (U.K.) for grant support (GR/G 63582) to MAG and studentship support to NESS.